Theoretical Investigation of the Kinetics for the Reactions of H with $GeH_{(4-n)}F_n$ ($n = 0, 1, 2, 3$)

Qingzhu Zhang, Shaokun Wang, and Yueshu Gu*

School of Chemistry and Chemical Engineering, Shandong University, Jinan 250100, P. R. China

Received: April 23, 2002; In Final Form: June 10, 2002

The direct hydrogen abstraction reactions of H atoms with GeH_4, GeH_3F, GeH_2F_2, and $GeHF_3$ have been studied systematically using ab initio molecular orbital theory. For all of the reactions, the potential energy surface information has been calculated at the MP2 level with the 6-311G(2d,p) basis set. Energies along the minimum energy path have been improved by a series of single-point ab initio G2MP2//MP2 calculations. Theoretical analysis provides conclusive evidence that the main process occurring in each case is the hydrogen abstraction from the Ge−H bond; the fluorine abstraction from the Ge−F bond has a higher barrier and is difficult to react. Changes of geometries, generalized normal-mode vibrational frequencies, and potential energies along the reaction path of the reactions are discussed and compared. The reaction thermal rate constants for the temperature range 200−3000 K are deduced by the canonical variational transition-state theory (CVT) with small-curvature tunneling (SCT) correction method. The calculated results show that the variational effect is small and that in the lower-temperature range the small curvature tunneling effect is important for all of the title reactions. The CVT/SCT rate constants exhibit typical non-Arrhenius behavior. Three-parameter rate−temperature formulas have been fitted as follows: $k_1 = 1.82 \times 10^{-17}T^{2.16} \exp(-282.56/T)$, $k_2 = 3.74 \times 10^{-18}T^{2.09} \exp(-368.21/T)$, $k_3 = 2.43 \times 10^{-20}T^{2.29} \exp(-412.36/T)$, and $k_4 = 1.38 \times 10^{-19}T^{2.25} \exp(-536.54/T)$ for the reactions of H with GeH_4, GeH_3F, GeH_2F_2, and $GeHF_3$, respectively (in units of cm^3 $molecule^{-1}$ s^{-1}). Studies show that the fluorine substitution has an effect on the strength and reactivity of the Ge−H bond in $GeH_{(4-n)}F_n$ ($n = 1-3$).

1. Introduction

Silanes and germanes are important reactants in chemical vapor deposition (CVD) used in the semiconductor industry.[1−4] The reactions with atomic hydrogen, the simplest free-radical species, are particularly interesting because these reactions provide an uncomplicated probe of chemical reactivity. In three previous contributions from this laboratory, we presented the kinetics properties and theoretical rate constants for the reactions of H with fluorosilanes,[5] chlorosilanes,[6] and methylgermanes.[7] As part of our ongoing work in this field, this paper investigates theoretically the kinetics properties of the reactions of H with GeH_4, GeH_3F, GeH_2F_2, and $GeHF_3$.

For the reaction of H with GeH_4, several experimental studies were reported. The early two studies performed by Choo et al.[8] and Austin and Lampe[9] produced conflicting results. In an attempt to adjudicate between them and to extend measurements to other temperatures, Nava et al.[10] and Arthur and Cooper[11] studied this reaction successively, and they obtained satisfactory agreements. Arthur and Cooper measured the rate constants in the temperature range of 293−473 K and combined his results with those of Nava et al. to give a best value for rate constants of $k = (1.21 \pm 0.10) \times 10^{-10} \exp(-1008 \pm 25)/T$ (in cm^3 $molecule^{-1}$ s^{-1}). Theoretically, three investigations are on record for this reaction. In 1975, Choo et al.[8] studied this reaction using the bond-energy bond-order (BEBO) method of Johnston[12] and found that the activation energy was overestimated with respect to the experimental data. In 1999, Espinosa-Garcia[13] constructed the potential energy surface of this reaction. Thermal- and vibrational-state-selected rate constants were obtained over the temperature range of 200−500 K. In 2000, Yu et al.[14] studied the reaction using ab initio molecular orbital theory combined with the canonical variational transition-state theory. The geometric parameters and frequencies were calculated at the QCISD/6-311+G(d,p) level, and the energies were calculated at the G2 theory. The rate constants were obtained over a temperature range of 200−1600 K; a three-parameter expression was fitted: $k = 2.0 \times 10^7 T^{2.12} \exp(-492)/T$ (in cm^3 mol^{-1} s^{-1}). It can be seen that the reaction of H with GeH_4 had ever been studied theoretically by Espinosa-Garcia and Yu et al. at much higher levels. We have studied this reaction for two purposes: (1) comparison with the reactions of H with fluorogermanes; (2) testing the reliability of our calculations.

However, for the reactions of H with GeH_3F, GeH_2F_2, and $GeHF_3$, the situation has been poorer still. To our best knowledge, little experimental and theoretical attention has been paid to these reactions.

Here, we present the first systematic and theoretical study on the reactions of atomic H with fluorogermanes. Several important features of this work are the following: (1) The reaction mechanisms have been revealed at high levels of ab initio molecular orbital theory. (2) The energy profile surfaces have been calculated at the G2MP2[15] theory level. (3) The kinetics nature has been studied in the temperature range from 200 to 3000 K using interpolated canonical variational transition-state theory (CVT) [16−18] and the centrifugal-dominant, small-curvature tunneling approximation (SCT),[19] including information at the reactants, products, transition states, and extra points along the minimum energy path. (4) The non-Arrhenius expres-

* To whom correspondence should be addressed. E-mail: guojz@icm.sdu.edu.cn.

10.1021/jp021035j CCC: $22.00 © 2002 American Chemical Society
Published on Web 09/11/2002

sions have been fitted. (5) The effect of fluorine substitution on the strength and the reactivity of the Ge−H bond has been discussed. Our theoretical results might be useful not only for further experimental measurements in the kinetics communities but also for computer-modeling studies directed toward obtaining an understanding of the factors controlling CVD processes.

2. Computation Methods and Theory

Ab initio calculations have been carried out using Gaussian 94 programs.[20] In the whole paper, MP2 and QCISD(T) denote the unrestricted versions, UMP2 and UQCISD(T). The geometries of the reactants, transition states, and products have been optimized at the MP2/6-311G(2d,p) level for all of the reactions. The vibrational frequencies have been calculated at the same level of theory to determine the nature of the stationary points, the zero-point energy (ZPE), and the thermal contributions to the free energy of activation. The intrinsic reaction coordinate (IRC) calculation confirms that the transition state connects the designated reactants and products. At the MP2/6-311G(2d,p) level, the minimum energy path (MEP) has been obtained with a gradient step size of 0.02 amu$^{1/2}$ bohr in mass-weighted Cartesian coordinates for each reaction. The force constant matrices of the stationary points and 30 selected nonstationary points (15 points in the reactant side and 15 points in the product side) near the transition state along the MEP have been also calculated for all of the reactions. To obtain accurate energies for the subsequent kinetics calculation, the single-point energies have been calculated at MP2, QCISD(T), and G2MP2 levels for the reaction of H with GeH_4. The largest basis set used in the above energy calculations is 6-311+G(3df,3pd). The G2MP2 method has been used for the reactions of H with fluorogermanes. It needs to be pointed that we have made two modifications in our G2MP2 calculations: (1) the geometries are obtained at the MP2/6-311G(2d,p) level instead of MP2-(FULL)/6-31G(d), and (2) the zero-point energy (ZPE) and vibrational frequencies are obtained at the MP2/6-311G(2d,p) level.

The initial information obtained from our ab initio calculations allowed us to calculate the variational rate constant including the tunneling effect. The canonical variational theory (CVT)[16−18] rate constant for temperature T is given by

$$k^{\mathrm{CVT}}(T) = \min_{s} k^{\mathrm{GT}}(T,s) \tag{1}$$

where

$$k^{\mathrm{GT}}(T,s) = \frac{\sigma k_{\mathrm{B}} T}{h} \frac{Q^{\mathrm{GT}}(T,s)}{\Phi^{\mathrm{R}}(T)} \mathrm{e}^{-V_{\mathrm{MEP}}(s)/(k_{\mathrm{B}}T)} \tag{2}$$

where, $k^{\mathrm{GT}}(T,s)$ is the generalized transition-state theory rate constant at the dividing surface s, σ is the symmetry factor accounting for the possibility of more than one symmetry-related reaction path, k_{B} is Boltzmann's constant, h is Planck's constant, $\Phi^{\mathrm{R}}(T)$ is the reactant partition function per unit volume, excluding symmetry numbers for rotation, and $Q^{\mathrm{GT}}(T,s)$ is the partition function of a generalized transition state at s with a local zero of energy at $V_{\mathrm{MEP}}(s)$ and with all rotational symmetry numbers set to unity. All of the kinetics calculations have been carried out using the POLYRATE 7.8 program.[21] The rotational partition functions were calculated classically, and the vibrational modes were treated as quantum-mechanical separable harmonic oscillators. Finally, we considered the tunneling effect correction. Because the heavy−light−heavy mass combination is not present in these hydrogen abstraction reactions, the tunneling correction is calculated using the centrifugal-dominant small-curvature tunneling approximation (SCT).[19]

TABLE 1: The Calculated Frequencies (in cm^{-1}) and the Zero-Point Energies (ZPE, in kcal/mol) for Reactants, Products, and Transition States Involved in the Reactions of H with $GeH_{(4-n)}F_n$ (n = 0, 1, 2, 3) at the MP2/6-311G(2d,p) Level

species	frequencies	ZPE
GeH_4	2228, 2228, 2228, 2221, 948, 948, 854, 854, 854 *2114, 2114, 2114, 2106, 946, 946, 834, 834, 834*	19.08
GeH_3F	2243, 2243, 2241, 906, 896, 895, 747, 653, 643 *2132, 2132, 2121, 874, 859, 859, 701, 643, 643*	16.41
GeH_2F_2	2282, 2272, 879, 841, 776, 764, 655, 602, 235 *2175, 2154, 860, 813, ∼720, 720*	13.30
$GeHF_3$	2324, 805, 805, 768, 723, 279, 226, 226	9.83
GeH_3	2208, 2208, 2185, 882, 881, 729	13.00
GeH_2F	2185, 2150, 855, 743, 738, 642	10.46
$GeHF_2$	2106, 763, 751, 668, 664, 229	7.40
SiF_3	783, 783, 744, 269, 214, 213	4.30
TS_1	2217, 2217, 2212, 1197, 956, 956, 880, 880, 815, 292, 292, 1450i	18.46
TS_2	2225, 2213, 1174, 952, 950, 873, 745, 720, 651, 285, 170, 1550i	15.67
TS_3	2228, 1185, 947, 930, 771, 756, 696, 657, 232, 189, 175, 1642i	12.53
TS_4	1207, 899, 899, 794, 794, 754, 272, 224, 224, 175, 175, 1691i	9.17

[a] The values in italics are the experimental data.[23−25]

TABLE 2: The Potential Barriers, ΔE (kcal/mol), and the Reaction Enthalpies, ΔH (kcal/mol), Calculated for the Reaction of H with GeH_4 at Various Theory Levels

theory level	ΔE	ΔH
MP2/6-311G(d)	6.62	−16.91
MP2/6−311gG(2d,p)	6.52	−17.06
MP2/6-311+G(3df,2p)	6.65	−18.33
QCISD(T)/6-311G(d,p)	4.12	−19.37
QCISD(T)/6-311+G(3df,2p)	3.03	−19.64
QCISD(T)/6-311+G(3df,3pd)	2.90	−19.68
G2MP2	3.16	−19.84
expt		−21.21
	2.53[a]	−21.41[a]
	3.54[b]	−19.22[b]

[a] The values were obtained from potential energy surface.[13] [b] The values were done at G2//QCISD/6-311+G(d,p) by Yu et al.[14]

TABLE 3: The Potential Barriers, ΔE (kcal/mol), Reaction Enthalpies, ΔH (kcal/mol), and the Ge−H Bond Dissociation Energies, $D_0(GeH_{(3-n)}F_n-H)$ (n = 0, 1, 2, 3) (kcal/mol), Calculated for the Hydrogen Abstraction Reactions of H with Germane and Fluorogermanes at the G2MP2//MP2/6-311G(2d,p) Level

reactions	ΔE	ΔH	D_0(Ge−H)
H + GeH_4	3.16	−19.84	84.01
H + GeH_3F	3.58	−18.89	84.96
H + GeH_2F_2	3.96	−18.70	85.14
H + $GeHF_3$	4.33	−16.82	87.03

3. Result and Discussion

The optimized geometries of reactants, transition states, and products are shown in Figure 1. The transition states of the reactions of H with GeH_4, GeH_3F, GeH_2F_2, and $GeHF_3$ are denoted as TS_1, TS_2, TS_3, and TS_4, respectively. The vibrational frequencies of reactants, products, and transition states are listed in Table 1. The potential barriers, ΔE, and the reaction enthalpies, ΔH, calculated are summarized in Table 2 for the reaction of H with GeH_4 and in Table 3 for the reactions of H with fluorogermanes. Figure 2 depicts the change curves of the

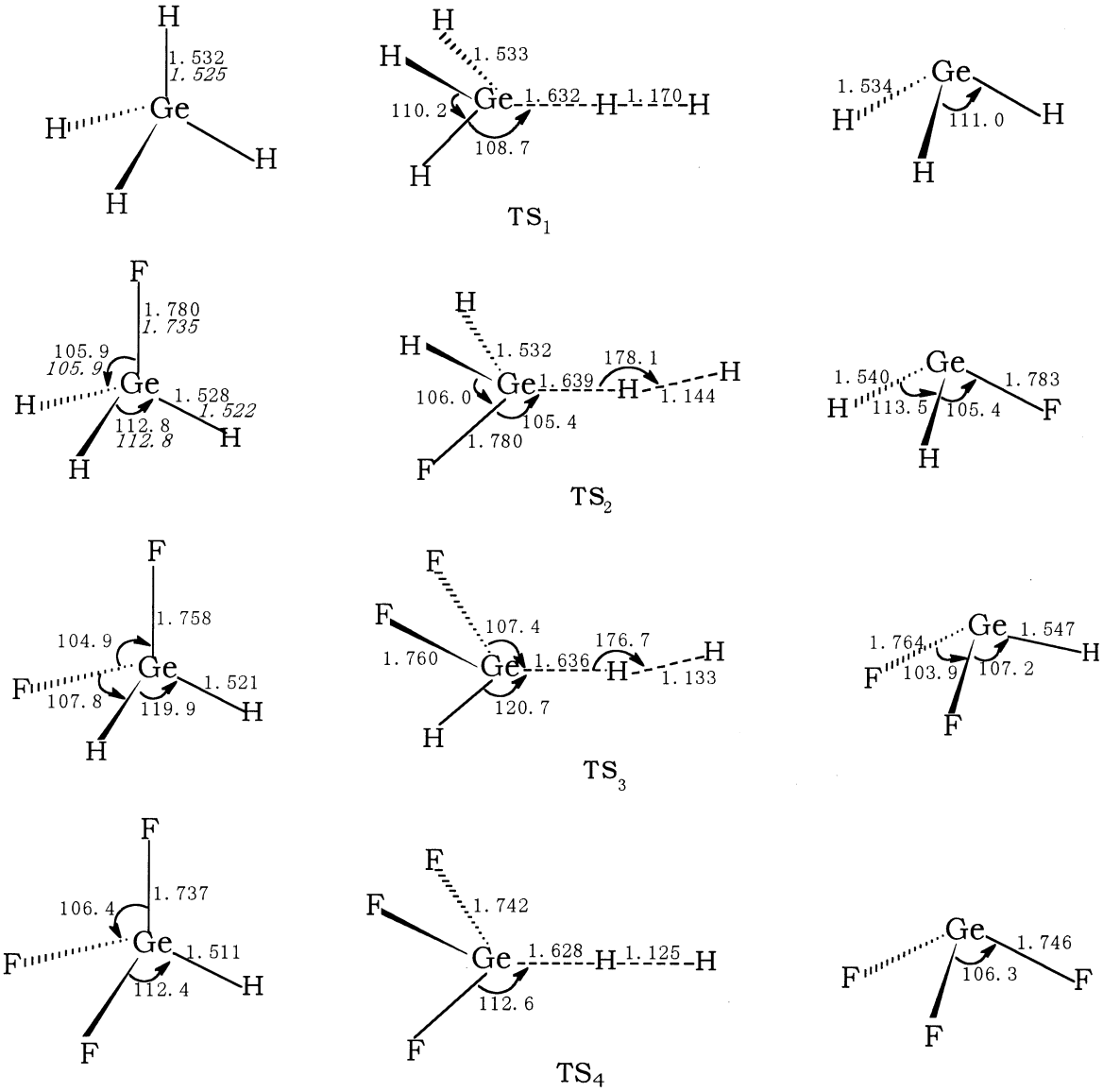

Figure 1. The optimized geometries for reactants, transition states, and products at the MP2/6-311G(2d,p) level. The values in italics are the experimental data.[22,23] The bond length is in Å, and the bond angle is in deg.

classical potential energy (V_{MEP}) and vibrationally adiabatic potential energy curves (V_a^G) with the reaction coordinate *s* at G2MP2//MP2/6-311G(2d,p) level for all of the reactions. Change curves of the generalized normal-mode vibrational frequencies with the reaction coordinate *s* are shown in Figure 3 for all of the reactions. The calculated TST, CVT, and CVT/SCT rate constants along with the experimental values are presented in Figure 4.

3.1. The Reaction Mechanism. As mentioned above, the reactions of H with GeH_3F, GeH_2F_2, and $GeHF_3$ can proceed via two channels: the hydrogen abstraction from the Ge−H bond and the fluorine abstraction from the Ge−F bond. The barrier heights calculated at the G2MP2 level are 3.58, 3.96, and 4.33 kcal/mol for the hydrogen abstraction from GeH_3F, GeH_2F_2, and $GeHF_3$, while the barrier heights of the fluorine abstraction are 26.26, 31.23, and 32.39 kcal/mol, respectively. The latter are much higher than the former. Thus, we can safely say that the fluorine abstraction is negligible for the reactions of H with GeH_3F, GeH_2F_2, and $GeHF_3$, which is very similar to the mechanism of the reactions of H with SiH_3F, SiH_2F_2, and $SiHF_3$.[5] Therefore, we mainly discuss the hydrogen abstraction from GeH_3F, GeH_2F_2, and $GeHF_3$ in the following study.

a. Geometry and Frequency. It is worth stating the reliability of the calculations in this work. Because unrestricted Hartree−Fock (UHF) reference wave functions are not spin eigenfunctions for open-shell species,[26] we monitored the expectation values of $\langle S^2 \rangle$ in the MP2 optimization. The values of $\langle S^2 \rangle$ are always in the range of 0.750−0.777 for doublets at MP2/6-311G(2d,p) level. After spin annihilation, the values of $\langle S^2 \rangle$ are 0.750, where 0.750 is the exact value for a pure doublet. Thus, spin contamination is not severe in the MP2/6-311G(2d,p) optimization for all of the title reactions. This suggests that a single-determinant reference wave function is suitable for the level of theory used in the optimization.

To clarify the general reliability of the theoretical calculations, it is useful to compare the predicated chemical properties of the present particular systems of interest with experimental data. As shown in Figure 1, the calculated geometric parameters of GeH_4 and GeH_3F are in good agreement with the available experimental values. From this result, it might be inferred that the same accuracy could be expected for the calculated transition-state geometries, but such an inference would be unjustified because transition states are much harder to calculate. As can be seen from Table 1, the vibrational frequencies of

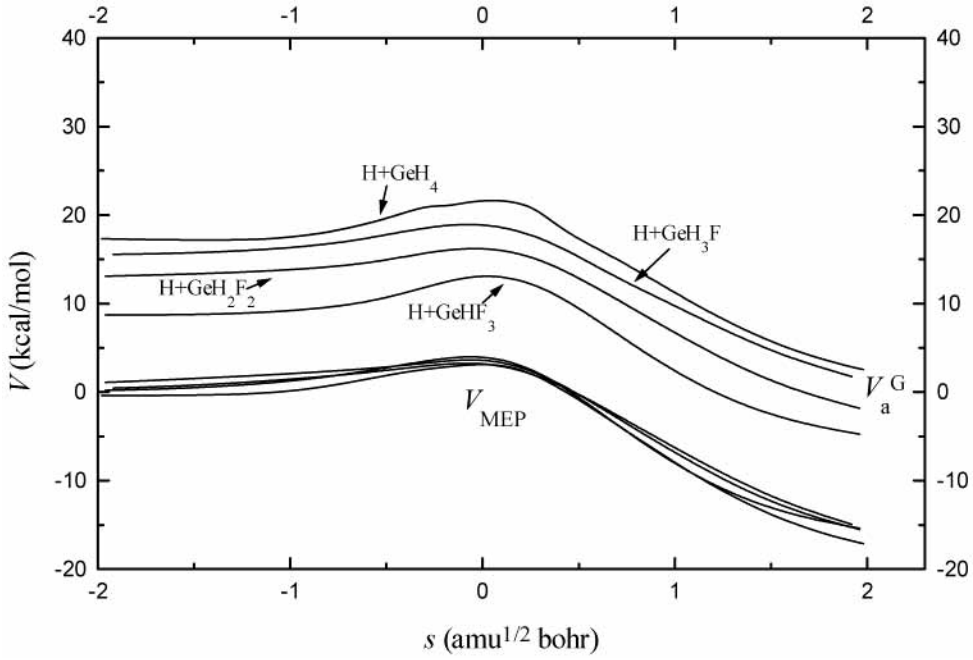

Figure 2. The classical potential energy (V_{MEP}) and the vibrationally adiabatic potential energy curves (V_a^G) as functions of s for the reactions of H with $GeH_{(4-n)}F_n$ ($n = 0, 1, 2, 3$) at the G2MP2//MP2/6-311G(2d,p) level.

GeH_4, GeH_3F, and GeH_2F_2 agree well with the experimentally observed fundamentals, and the maximum relative error is less than 6.5%. These good agreements give us confidence that the MP2/6-311G(2d,p) theory level is adequate to optimize the geometries and calculate the frequencies.

The transition states of the hydrogen abstraction from GeH_4, GeH_3F, GeH_2F_2, and $GeHF_3$ are denoted as TS_1, TS_2, TS_3, and TS_4, respectively. Their geometrical parameters calculated at the MP2/6-311G(2d,p) level are shown in Figure 1. For the reactions of H with GeH_4 and $GeHF_3$, the H atom attacks linearly the H of the Ge−H bond, and the transition states TS_1 and TS_4 have C_{3v} symmetry. For the reactions of H with GeH_3F and GeH_2F_2, the H atom attacks one H of Ge−H bonds with a slightly bent orientation angle of 178.1° and 176.7°, respectively. Thus, the transition states TS_2 and TS_3 have C_s symmetry. For the transition states TS_1, TS_2, TS_3, and TS_4, the breaking Ge−H bonds are elongated by 6.53%, 7.26%, 7.56%, and 7.74%, while the forming H−H bonds are longer than the equilibrium value of 0.738 Å in H_2 by 58.54%, 55.01%, 53.52%, and 52.44%, respectively. Therefore, TS_1, TS_2, TS_3, and TS_4 are reactant-like, and the hydrogen abstraction reactions from germane and fluorogermanes proceed via early transition states. This rather early character in these transition states is in accordance with the low reaction barrier and the high exothermicity of these reactions, in keeping with Hammond's postulate.[27] For the reaction of GeH_4 and H, our theoretical result is compared with that of Espinosa-Garcia[13] and Yu et al.[14] In the transition-state structure located by Espinosa-Garcia, the breaking Ge−H bond increases by 5.18% with respect to the equilibrium bond length of GeH_4, while the forming H−H bond is elongated by 63.61%. In the transition-state structure located by Yu et al. at QCISD/6-311G(d,p) level, the breaking Ge−H bond is stretched by 5.18%, while the forming H−H bond is elongated by 68.79%. Both of them indicate the reaction of GeH_4 and H proceeds via an early transition state, which is in accordance with our theoretical result.

Table 1 shows that transition states of the hydrogen abstraction from GeH_4, GeH_3F, GeH_2F_2, and $GeHF_3$ have one and only one imaginary frequency. The values of the imaginary frequencies are large, which implies that the quantum tunneling effect may be significant and may play an important role in the calculation of the rate constant.

b. Energy. To choose a reliable theory level to calculate the energy, we calculated potential barriers, ΔE, and the reaction enthalpies, ΔH, at various levels of theory for the reaction of H with GeH_4. The values were listed in Table 2. First, we analyze the reaction enthalpy. Espinosa-Garcia[13] obtained a better experimental value of −21.21 kcal/mol from the measured $\Delta H_{f,0}$ for GeH_4, GeH_3, and H. The values calculated at the MP2 level with different basis sets are in great disagreement with this experimental value; similar calculation with the highly correlated and more computationally demanding G2MP2 and QCISD(T) levels predict the values that are in excellent agreement with the experimental result, especially if the experimental uncertainty for GeH_3 (±2 kcal/mol) is taken into consideration. These results clearly indicated that most of the error in the reaction enthalpy computed at the MP2 level can be attributed to the lack of correlation in such method and not to an improper optimized geometry at the MP2/6-311G(2d,p) level.

It can be seen from Table 2 that the potential barriers have a great discrepancy obtained at different levels. The values calculated at the MP2 level with different basis sets are greater than those obtained at the highly correlated and more computationally demanding QCISD(T) level. The value calculated at QCISD(T) level with 6-311G(d,p) basis set is greater by about 1 kcal/mol than that calculated at the same level with 6-311+G(3df,2p) and 6-311+G(3df,3pd) basis sets; this means that the size of the basis set will have an important effect on the potential barrier calculated. The value calculated at G2MP2 level is in good agreement with the values calculated at QCISD(T)/6-311+G(3df,2p) and at QCISD(T)/6-311+G(3df,3pd) levels, while the computational time and demand of the G2MP2 are much less than that of the QCISD(T)/6-311+G(3df,2p) and QCISD(T)/6-311+G(3df,3pd). The objective of the study of the reaction of H with GeH_4 is to develop an inexpensive method that can be applied to fluorogermanes, especially to $GeHF_3$.

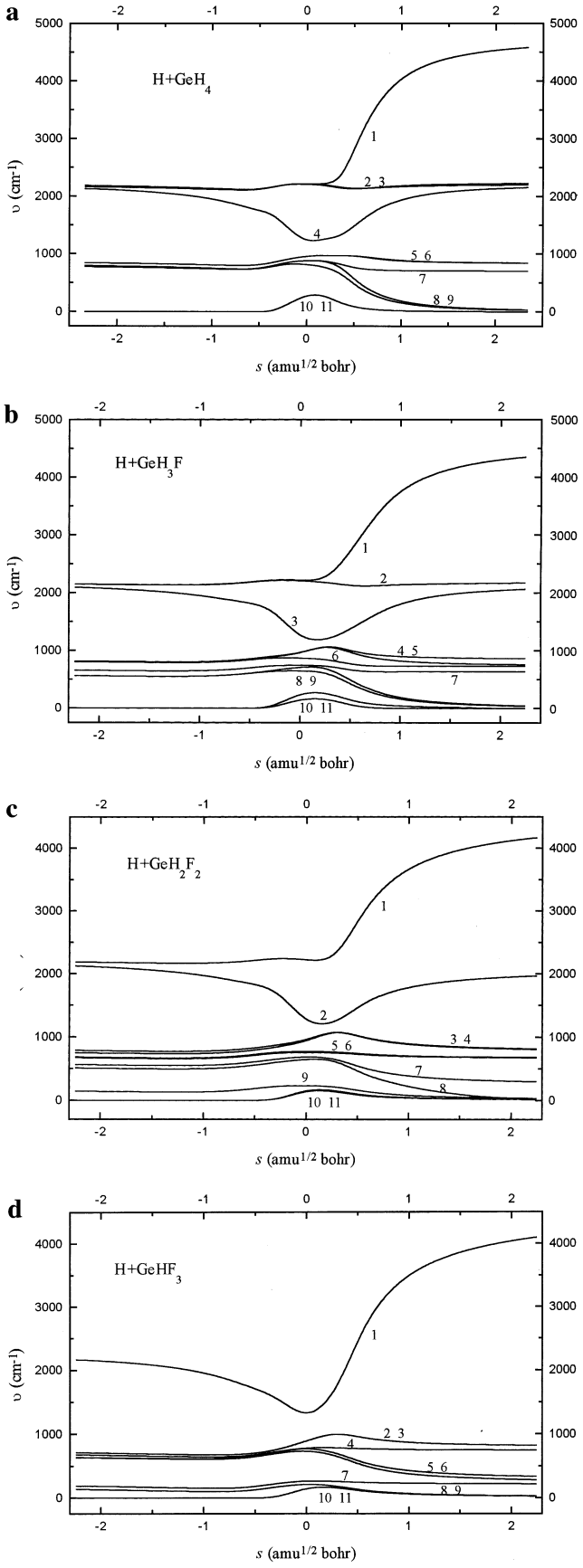

Figure 3. Changes of the generalized normal-mode vibrational frequencies as functions of s at the MP2/6−311(2d,p) level for the reactions of H with $GeH_{(4-n)}F_n$ (n = 0, 1, 2, 3).

Thus, although QCISD(T)/6-311+G(3df,2p) and QCISD(T)/6-311+G(3df,3pd) levels result in better values of the potential barrier, they are too computationally intensive to be generally applicable for the reactions of H with fluorogermanes at the present time. Therefore, in this work, we have chosen the

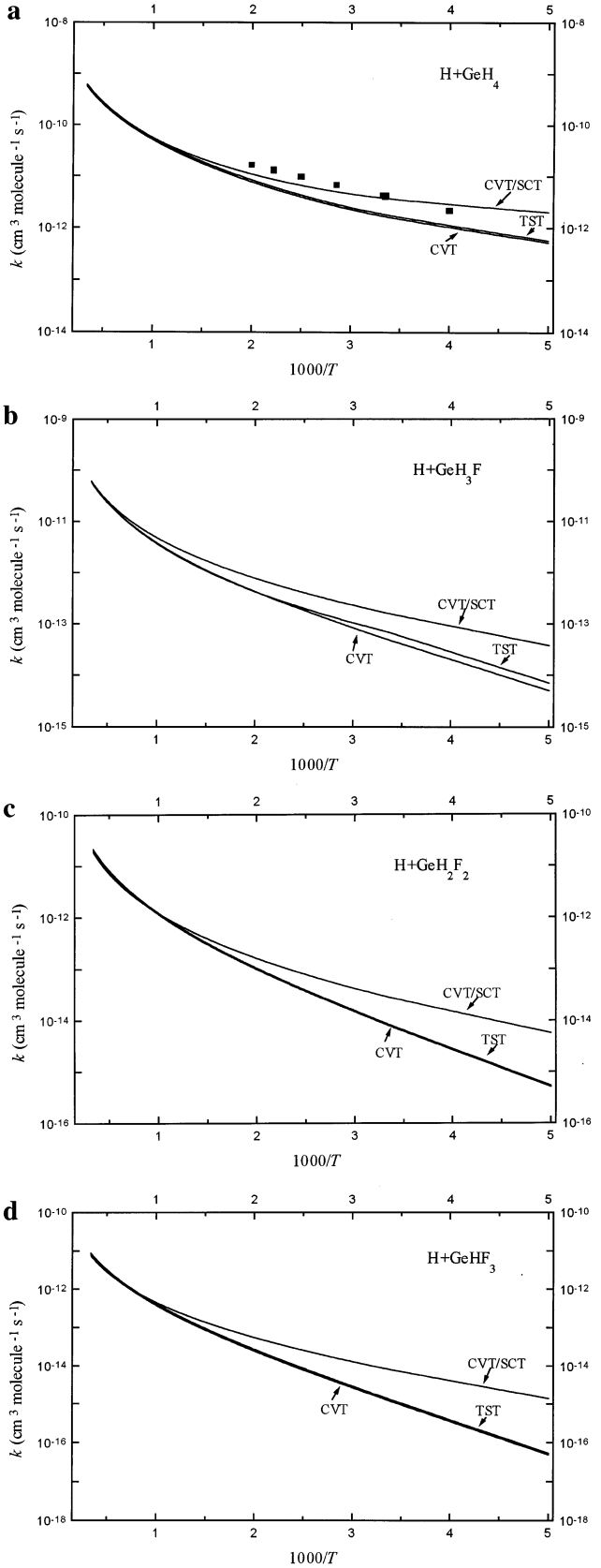

Figure 4. Rate constants as function of the reciprocal of the temperature (K) over the temperature range of 200−3000 K for the reactions of H with $GeH_{(4-n)}F_n$ (n = 0, 1, 2, 3). The symbols (■) are the experimental values.[11]

G2MP2 method to calculate the potential barriers and the reaction enthalpies for the reactions of H with fluorogermanes.

It is worth discussing the effect of fluorine substitution on the geometrical parameters and the reaction mechanism for the reactions of H with GeH_4, GeH_3F, GeH_2F_2, and $GeHF_3$. There are four features for the four reactions. First, the Ge−H bond length in GeH_4 is 1.532 Å at the MP2/6-311G(2d,p) level, while the Ge−H bond lengths are 1.528, 1.521, and 1.511 Å in GeH_3F, GeH_2F_2, and $GeHF_3$. There is a slight decrease in Ge−H bond length along the series from GeH_4 to $GeHF_3$. Second, the potential barrier of the reaction of H with GeH_4 is 3.16 kcal/mol at the G2MP2 level, while the potential barriers of the reactions of H with GeH_3F, GeH_2F_2, and $GeHF_3$ are 3.58, 3.96, and 4.33 kcal/mol, respectively. The reaction of H with GeH_4 possesses the lowest potential barrier. The potential barriers of the reactions of H with fluorogermanes are 0.42−1.17 kcal/mol higher than that of the H with GeH_4 reaction. The higher the number of fluorine substitutions is, the higher barrier the reaction will have, which means that hydrogen abstraction from fluorogermanes is more difficult than from GeH_4 and the fluorine substitutions decrease the reactivity of the Ge−H bond. The following study of the rate constants further testifies to this view. Third, the reaction enthalpy of the reaction of H with GeH_4 is −19.84 kcal/mol at the G2MP2 level, while the values for the reactions of H with GeH_3F, GeH_2F_2, and $GeHF_3$ are −18.89, −18.70, and −16.82 kcal/mol. The exothermicities of the reactions of H with fluorogermanes are less than that of H with GeH_4, and the exothermicity decreases with the increase in fluorine substitution from GeH_3F to $GeHF_3$ through GeH_2F_2. The reaction barriers increase in the same order. This observation is in accord with the suggestion of Evans and Polanyi.[28] They pointed out that the barrier heights for atom transfer reactions should increase with the decrease in exothermicity. Fourth, the dissociation energy of the Ge−H bond in the GeH_4 is 84.01 kcal/mol at the G2MP2 level, while dissociation energies of Ge−H bonds in the GeH_3F, GeH_2F_2, and $GeHF_3$ are 84.96, 85.14 and 87.03 kcal/mol, respectively. There is an increase in Ge−H bond dissociation energies along the series from GeH_4 to $GeHF_3$. The above analysis suggests that fluorine substitutions have a noticeable effect on the reactivity and the strength of the Ge−H bond. The following kinetics study further testifies to this view.

3.2. The Kinetics Calculation. *a. Reaction Path Properties.* With a step size of 0.05 $amu^{1/2}$ bohr, the intrinsic reaction coordinate (IRC) has been calculated at the MP2/6-311G(2d,p) level from the transition state to the reactants and the products for each reaction. For the reaction of H with GeH_3F, the breaking Ge−H bond is almost unchanged from $s = -\infty$ to $s = -0.5$ $amu^{1/2}$ bohr and equals the value in the reactant and stretches linearly after $s = -0.5$ $amu^{-1/2}$ bohr. The forming H−H bond shortens rapidly from reactants and reaches the equilibrium bond length in H_2 at $s = 0.5$ $amu^{1/2}$ bohr. Other bond lengths are almost unchanged during the reaction process. Therefore, the transition state TS_2 connects the reactants (GeH_3F and H) with the products (GeH_2F and H_2). The geometric change mainly takes place in the region from $s = -0.5$ to $s = 0.5$ $amu^{1/2}$ bohr. The same conclusion can be drawn from the reactions of H with GeH_4, GeH_2F_2, and $GeHF_3$.

The minimum energy path (MEP) is calculated at the MP2/6-311G(2d,p) level by the IRC definition with a step size of 0.02 $amu^{1/2}$ bohr, and the energies of the MEP are further refined by the G2MP2//MP2 method. For all of the reactions, the maximum position of the classical potential energy curve, V_{MEP}, at the G2MP2//MP2/6-311G(2d,p) level corresponds to the saddle-point structure at the MP2/6-311G(2d,p) level. Therefore, the shifting of the maximum position for the V_{MEP} curve caused by the computational technique is avoided.[29] The changes of the classical potential energy, V_{MEP}, and the ground-state vibrational adiabatic potential energy, V_a^G, with the reaction coordinate s are shown in Figure 2 for the reactions of H with GeH_4, GeH_3F, GeH_2F_2, and $GeHF_3$. It is interesting to note that the change trend of V_{MEP} and V_a^G are similar for these four reactions; this means that they have similar reaction mechanism. It can be also seen from Figure 2 that the maximum positions of V_{MEP} and V_a^G energy curves are almost the same at the G2MP2//MP2 level for each reaction. The zero-point energy, ZPE, which is the difference of V_a^G and V_{MEP}, is almost unchanged as s varies. This means that the variational effect will be small for the four reactions. To analyze this behavior in greater detail, we show the variation of the generalized normal modes vibrational frequencies as functions of s in Figure 3 for all of the reactions.

Along the MEP, a generalized normal-mode analysis has been performed using reactilinear Cartesian coordinate for each reaction. In the negative limit of s, the frequencies are associated with the reactants, while in the positive limit of s, the frequencies are associated with the products. For the sake of clarity, the vibrational frequencies can be divided into three types: spectator modes, transitional modes, and reactive modes. The spectator modes are those that undergo little change and sometimes remain basically unchanged in going from reactants to the transition state. The transitional modes appear along the reaction path as a consequence of the transformation from free rotation or free translations within the reactant or the product limit into real vibrational motions in the global system. Their frequencies tend to zero at the reactant and the product limit and reach their maximum in the saddle-point zone. The reactive modes are those that undergo the largest change in the saddle-point zone, and therefore, they must be related to the breaking/forming bonds. The mode (mode 4 for H + GeH_4, mode 3 for H + GeH_3F, mode 2 for H + GeH_2F_2, and mode 1 for H + $GeHF_3$, respectively) that connects the frequency of the Ge−H stretching vibration of the reactant with the frequency of the H−H stretching vibration of H_2 is the reactive mode. Modes 10 and 11 are transitional modes, and other modes are spectator modes. From $s = -0.5$ to $s = 1.0$ $amu^{1/2}$ bohr for the reactions of H with GeH_4, GeH_3F, and GeH_2F_2 and from $s = -1.0$ to $s = 1.0$ $amu^{1/2}$ bohr for the reaction of H with $GeHF_3$, the reactive mode drops dramatically; this behavior is similar to that found in other hydrogen abstraction reactions.[30−32] A priori, this drop should cause a considerable fall in the zero-point energy near the transition state. But because this kind of drop of the reactive mode is compensated by the transitional modes, the zero-point energy shows very little change with the change of the reaction coordinate s for all of the reactions.

b. The Rate Constants. Canonical variational transition-state theory (CVT) with small-curvature tunneling correction (SCT), which has been successfully performed for several analogous reactions,[5−7] is an effective method to calculate the rate constants. In this paper, we used this method to calculate the rate constants for the reactions of H with GeH_4, GeH_3F, GeH_2F_2, and $GeHF_3$ over a wide temperature range from 200 to 3000 K.

To calculate the rate constants, 30 points are selected near the transition state along the MEP for each reaction, 15 points in the reactant side and 15 points in the product side. The calculated CVT/SCT rate constants along with the experimental values are shown in Figure 4 for these four reactions. The calculated TST and CVT are also depicted in Figure 4 for comparison purposes. Several important features of the calcu-

lated rate constants are the following: (1) For the four reactions, the TST rate constants and the CVT rate constants are almost the same over the whole studied temperature range, which enables us to conclude that the variational effect is small for the calculation of the rate constant. (2) Reactions involving hydrogen atom transfer are usually characterized by significant tunneling effect that must be accounted for when computing reaction rate constants. For all of the reactions, the CVT/SCT rate constants are greater than the CVT ones over the temperature range of 200−1000 K. However, when the temperature is higher than 1000 K, the CVT/SCT rate constants are asymptotic to the rate constants of CVT, which means only in the lower temperature range the small curvature tunneling correction plays an important role for the calculation of the rate constant. (3) For the reaction of GeH_4 and H, the calculated CVT/SCT rate constants are in excellent agreement with the experimental values over the temperature range of 293−473 K. Therefore, the CVT/SCT method is a good choice to calculate accurate rate constants for the title systems. Both the TST method and the CVT method without the tunneling effect correction underestimate rate constants. Because the reactions of H with germane and fluorogermanes have similar reaction mechanisms, the CVT/SCT rate constants for the reactions of H with fluorogermanes (namely, GeH_3F, GeH_2F_2, and GeH_3F) are expected to have similar accuracy. (4) It is obvious that the CVT/SCT rate constants exhibit typical non-Arrhenius behavior. The CVT/SCT rate constants of the title reactions are fitted by three-parameter formulas over the temperature range of 200−3000 K and given in units of cm^3 $molecule^{-1}$ s^{-1} as follows:

$$k_1 = 1.82 \times 10^{-17} T^{2.16} \exp(-282.56/T) \quad \text{for} \quad \text{H with } GeH_4$$

$$k_2 = 3.74 \times 10^{-18} T^{2.09} \exp(-368.21/T) \quad \text{for} \quad \text{H with } GeH_3F$$

$$k_3 = 2.43 \times 10^{-20} T^{2.29} \exp(-412.36/T) \quad \text{for} \quad \text{H with } GeH_2F_2$$

$$k_4 = 1.38 \times 10^{-19} T^{2.25} \exp(-536.54/T) \quad \text{for} \quad \text{H with } GeHF_3$$

(5) The effect of fluorine substitution on the reactivity of the Ge−H bond can be seen by evaluating the room-temperature *k/n*, the room-temperature rate constant corrected for the reaction-path degeneracy, where *n* is the number of the Ge−H bonds. At 298 K, the *k/n* for the reaction of H with GeH_4 is 4.00×10^{-13} cm^3 $molecule^{-1}$ s^{-1}; for the reactions of H with GeH_3F, GeH_2F_2, and $GeHF_3$, the values of *k/n* are 5.37×10^{-14}, 1.41×10^{-14}, and 8.39×10^{-15} cm^3 $molecule^{-1}$ s^{-1}, respectively. It can be shown that the fluorine substitution decreases the reactivity of the Ge−H bond, which is reasonable in view of the Ge−H bond dissociation energies in $GeH_{(4-n)}F_n$ lying 0.95−3.02 kcal/mol above the Ge−H bond dissociation energy in GeH_4 at 0 K.

4. Conclusion

In this paper, we have studied systematically the reactions of H with GeH_4, GeH_3F, GeH_2F_2, and $GeHF_3$ using ab initio and canonical variational transition-state theory (CVT) with small-curvature tunneling effect. Both the reaction mechanism and the rate constants were reported over the temperature range of 200−3000 K. Several major conclusions can be drawn from this calculation. (1) The four title reactions have similar reaction mechanism. The transition states involved in these reactions have rather early character. (2) For the reactions of H with fluorogermanes, the hydrogen abstraction from the Ge−H bond is the sole channel. (3) The calculated CVT/SCT rate constants exhibit typical non-Arrhenius behavior. (4) Fluorine substitution increases the strength and decreases the reactivity of the Ge−H bond in $GeH_{4-n}F_n$ ($n = 1-3$).

Acknowledgment. The authors thank Professor Donald G. Truhlar for providing the POLYRATE 7.8 program. This work is supported by the Research Fund for the Doctoral Program of Higher Education of China.

References and Notes

(1) Doyle, J. R.; Doughty, D. A.; Gallagher, A. *J. Appl. Phys.* **1991**, *69*, 4169.
(2) Beaucarne, G.; Poortmans, J.; Caymax, M.; Nijs, J.; Mertens, R. *Mater. Res. Soc. Symp. Proc.* **1998**, *485*, 89.
(3) Koinuma, H.; Manako, T.; Natsuaki, H.; Fujioka, H.; Fueki, K. *J. Non-Cryst. Solids* **1985**, *77*, 801.
(4) Doyle, J. R.; Doughty, D. A.; Gallagher, A. *J. Appl. Phys.* **1992**, *71*, 4727.
(5) Zhang, Q.-Z.; Wang, S.-K.; Wang, C.-S.; Gu, Y.-S. *Phys. Chem. Chem. Phys.* **2001**, *3*, 4280.
(6) Zhang, Q.-Z.; Wang, S.-K.; Gu, Y.-S. *J. Phys. Chem. A* **2002**, *106*, 3796.
(7) Zhang, Q.-Z.; Zhang, D.-J.; Wang, S.-K.; Gu, Y.-S. *J. Phys. Chem. A* **2002**, *106*, 122.
(8) Choo, K. Y.; Gaspar, P. P.; Wolf, A. P. *J. Phys. Chem.* **1975**, *79*, 1752.
(9) Austin, E. R.; Lampe, F. W. *J. Phys. Chem.* **1977**, *81*, 1134.
(10) Nava, D. F.; Payne, W. A.; Marston, G.; Stief, L. J. *J. Geophys. Res.* **1993**, *98*, 5331.
(11) Arthur, N. L.; Cooper, I. A. *J. Chem. Soc., Faraday Trans.* **1995**, *91*, 3367.
(12) Johnston, H. S. *Gas-Phase Reaction Rate Constant*; Ronald: New York, 1965.
(13) Espinosa-Garcia, J. *J. Chem. Phys.* **1999**, *111*, 9330.
(14) Yu, X.; Li, S.-M.; Sun, C.-C. *J. Phys. Chem. A* **2000**, *104*, 9207.
(15) Curtiss, L. A.; Raghavachari, K.; Pople, J. A. *J. Chem. Phys.* **1993**, *98*, 1293.
(16) Baldrige, K. K.; Gordor, M. S.; Steckler, R.; Truhlar, D. G. *J. Phys. Chem.* **1989**, *93*, 5107.
(17) Gonzalez-Lafont, A.; Truong, T. N.; Truhlar, D. G. *J. Chem. Phys.* **1991**, *95*, 8875.
(18) Garrett B. C.; Truhlar, D. G. *J. Phys. Chem.* **1979**, *83*, 1052.
(19) Liu, Y.-P.; Lynch, G. C.; Truong, T. N.; Lu, D.-H.; Truhlar, D. C.; Garrett, B. C. *J. Am. Chem. Soc.* **1993**, *115*, 2408.
(20) Frisch, M. J.; Trucks, G. W.; Schlegel, H. B.; Gill, P. M. W.; Johnson, B. G.; Robb, M. A.; Cheeseman, J. R.; Keith, T.; Petersson, G. A.; Montgomery, J. A.; Raghavachari, K.; Al-Laham, M. A.; Zakrzewski, V. G.; Ortiz, J. V.; Foresman, J. B.; Cioslowski, J.; Stefanov, B. B.; Nanayakkara, A.; Challacombe, M.; Peng, C. Y.; Ayala, P. Y.; Chen, W.; Wong, M. W.; Andres, J. L.; Replogle, E. S.; Gomperts, R.; Martin, R. L.; Fox, D. J.; Binkley, J. S.; Defrees, D. J.; Baker, J.; Stewart, J. P.; Head-Gordon, M.; Gonzalez, C.; Pople, J. A. *Gaussian 94*, revision E.1; Gaussian, Inc.: Pittsburgh, PA, 1995.
(21) Steckler, R.; Chuang, Y. Y.; Fast, P. L.; Corchade, J. C.; Coitino, E. L.; Hu, W. P.; Lynch, G. C.; Nguyen, K.; Jackells, C. F.; Gu, M. Z.; Rossi, I.; Clayton, S.; Melissas, V.; Garrett, B. C.; Isaacson, A. D.; Truhlar, D. G. *POLYRATE*, 7.8 version; University of Minnesota: Minneapolis, MN, 1997.
(22) Cradock, S.; McKean, D. C.; MacKenzie, M. W. *J. Mol. Struct.* **1981**, *74*, 265.
(23) Lide, D. R. *CRC Handbook of Chemistry and Physics*, 79th ed.; CRC Press: New York, 1998.
(24) Freeman, D. E.; Rhee, K. H.; Wilson, M. K. *J. Chem. Phys.* **1963**, *39*, 2908.
(25) Ebsworth, E. A. V.; Robiette, A. G. *Spectrochim. Acta* **1964**, *20*, 1639.
(26) Liu, R.; Francisco, J. S. *J. Phys. Chem. A* **1998**, *102*, 9869.
(27) Hammmond, G. S. *J. Am. Chem. Soc.* **1955**, *77*, 334.
(28) Evans, M. G.; Polanyi, M. *Trans. Faraday Soc.* **1938**, *34*, 11.
(29) Espinosa-Garcia, J.; Corchado, J. C. *J. Phys. Chem.* **1995**, *99*, 8613.
(30) Truhlar, D. G.; Isaacson, A. D. *J. Chem. Phys.* **1982**, *77*, 3516.
(31) Espinosa-Garcia, J.; Corchado, J. C. *J. Phys. Chem.* **1996**, *100*, 16561.
(32) Corchado, J. C.; Espinosa-Garcia, J. *J. Chem. Phys.* **1997**, *106*, 4013.